Effect of various dopant elements on primary graphite growth

Nathalie Valle, Koenraad Theuwissen, Jon Sertucha, Jacques Lacaze

Effect of various dopant elements on primary graphite growth

N Valle[1], K Theuwissen[2], J Sertucha[3] and J Lacaze[2]*
[1] Department "Science and Analysis of Materials" (SAM), Centre de Recherche Public-Gabriel Lippmann 41 rue du Brill, 4422 Belvaux, Luxembourg.
[2] CIRIMAT, Université de Toulouse, ENSIACET, 31432 Toulouse cedex 4, France.
[3] Engineering and Foundry Processes Department, AZTERLAN, Aliendalde Auzunea 6, E-48200 Durango (Bizkaia), Spain.

E-mail: jacques.lacaze@ensiacet.fr

Abstract. Five spheroidal graphite cast irons were investigated, a usual ferritic grade and four pearlitic alloys containing Cu and doped with Sb, Sn and Ti. These alloys were remelted in a graphite crucible, leading to volatilization of the magnesium added for spheroidization and to carbon saturation of the liquid. The alloys were then cooled down and maintained at a temperature above the eutectic temperature. During this step, primary graphite could develop showing various features depending on the doping elements added. The largest effects were that of Ti which greatly reduces graphite nucleation and growth, and that of Sb which leads to rounded agglomerates instead of lamellar graphite. The samples have been investigated with secondary ion mass spectrometry to enlighten distribution of elements in primary graphite. SIMS analysis showed almost even distribution of elements, including Mg and Al (from the inoculant) in the ferritic grade, while uneven distribution was evident in all doped alloys. Investigations are going on to clarify if the uneven distribution is associated with structural defects in the graphite precipitates.

1. Introduction

Graphite in cast irons may adopt various shapes depending partly on casting conditions (cooling rate) but mainly on the presence of additives or of trace elements. It is generally agreed that oxygen and sulphur dissolved in a cast iron melt lead to lamellar graphite (LG). Adding 0.025 to 0.050 wt. % Mg (or Mg associated with Ce) insures in most cases that graphite precipitates as spheroids (SG), while a slightly smaller amount of Mg (0.009-0.018 wt. %) leads to compacted graphite. Further, associating Te and S is known to totally hinder graphite formation, while many other elements when present even as traces lead to degenerate forms of graphite such as chunky graphite. Values of maximum permissible contents for SG irons have been reviewed since long, e.g. by Lux [1]. Following a previous similar work [2], Javaid and Loper [3] sorted the elements affecting spheroidal graphite as elements that:

- reduce the effective Mg content by reacting with it, e.g. O, S, Se, Te, Ti, though the effect of Ti should be more complex as it does not form compounds with Mg;
- alter graphite growth, e.g. Al, As, Bi, Cd, Cu, Pb, Sb, Sn, with Bi and Pb that can also react with Mg;
- promote chunky graphite, e.g. Ce and Ca.

However, the detailed description made by the authors shows that this sorting is oversimplified because: i) some elements may be beneficial at low level and detrimental at higher level; ii) interaction has been evidenced; and iii) the effects may depend on casting conditions. Sn and Sb are examples of

elements that are reported as altering spheroidal growth in light-section castings while they offset the formation of chunky graphite in heavy section SG castings [4].

Following Francis [5], it may be considered to be very unlikely that heterogeneous graphite nuclei exert any influence on the final graphite shape which should be controlled by graphite growth conditions. Looking at the role of graphite modifiers, interest has been put on graphite chemistry as it may be expected that modifiers get incorporated into the graphite lattice. For such a purpose, the most usual means as electron probe or energy dispersive analyzers have often too poor detection limits. Francis [5] used chemical analysis of extracted graphite and reported that many elements could be detected in graphite. Auger electron spectroscopy (AES) has also been used but most generally gives only information on the interface and not the bulk of the phases. Though proton emission has been used successfully [6, 7], the most potential means appears to be secondary ion mass spectrometry (SIMS) that has already been used by a few authors [8, 9].

In an attempt to enlighten the effect of additives and trace elements on graphite growth, experiments have been carried out on a base ferritic cast iron and four pearlitic grades with about 1 wt.% Cu added and doped with Sb, Sn and Ti. These alloys have been remelted and resolidified in graphite crucibles so as to saturate the melt in carbon, much in line with the work by Patterson, Geilenberg and Lange [10, 11]. Solidification was performed in two steps, a slow cooling and holding above the eutectic temperature during which primary graphite formed, followed by a faster cooling during which the remaining of the melt solidified with a fine structure. Primary graphite precipitates have been characterized by optical and scanning electron microscopy and analyzed with SIMS.

2. Experimental details

All melts were prepared in 50 kg batches using a medium frequency induction furnace (250 Hz, 100 kW) 100 kg in capacity. The metallic charges were composed of 30-50% automotive steel scrap and 70-50% low alloyed pig iron. In the case of the ferritic alloy, no addition was made while extra additions of Cu, FeMn, FeTi, Sn and/or Sb were done to adjust the chemical composition to the targeted one for the pearlitic grades. After melting, the carbon and silicon contents were checked and adjusted when necessary. The liquid metal temperature was then increased to 1500-1510ºC and its surface skimmed. Nodularizing treatment was made by the sandwich method and using a 50 kg capacity ladle at the bottom of which was placed 1.3 wt.% of a FeSiMg alloy (42-44 wt.% Si, 5-6 wt.% Mg, 0.9-1.0 wt.% Ca, 0.4-0.5 wt.% Al, 0.9-1.1 wt.% RE). The treatment temperature was between 1470 and 1490ºC. When the reaction was finished, the alloy was cast in chemically bonded sand mold that contained standard keel-blocks as described elsewhere [12]. Inoculation was carried out by adding approximately 0.15% of a commercial inoculant (68.1 wt.% Si, 0.89 wt.% Al, 1.65 wt.% Ca, 0.45 wt.% Bi, 0.38 wt.% Ba, 0.37 wt.% RE) into the cavity of the molds. The final composition of the alloys is listed in Table 1. Some additional elements were found in some of the melts: B: 0.0059 wt.% in the ferritic alloy, none measured in the pearlitic ones; Cr: 0.03 wt.% in 8P1 and 8P3, none in the other three alloys; Zr, very low level, at most 0.005 wt.% in 9P3; Mo: 0.01 wt.% in all four pearlitic alloys.

Table 1. Composition of the investigated alloys (doping elements are in bold).

Alloy	C	Si	Mn	P	S	Mg	**Cu**	**Ti**	Al	N	Ni	other
10F2	3.64	2.05	0.11	0.033	0.015	0.037	**0.04**	**---**	---	0.0050	0.03	0.003 Bi
8P1	3.73	2.42	0.45	0.035	0.015	0.033	**0.95**	**---**	0.010	0.0041	0.02	**0.005 Sn**
8P3	3.49	2.60	0.40	0.035	0.015	0.033	**0.86**	**---**	0.006	0.0047	0.02	**0.024 Sn**
9P3	3.52	2.24	0.82	0.038	0.012	0.035	**1.08**	**0.022**	0.011	0.0038	0.04	**0.005 Sb**
12P3	3.65	1.98	0.37	0.026	0.013	0.039	**0.85**	**0.36**	<0.010	0.0033	0.07	**---**

These alloys were remelted in graphite crucibles by heating to 1300°C, leading to volatilization of the magnesium added for spheroidization and to carbon saturation of the liquid. After 10 min holding,

they were cooled to 1180°C in about 10 min and maintained at that temperature for 20 min. During this step, primary graphite precipitates were expected to nucleate and grow along the crucible walls. Finally, the crucible was extracted from the furnace which led to rapid solidification of the remaining melt. The samples were then cut vertically, and the section was polished and cleaned for metallographic observation, including optical and scanning electron (SEM) microscopy.

The SIMS analyses were performed on a modified CAMECA IMS-6f equipped with a gallium liquid metal ion gun. Although the Ga^+ source allows reaching a good lateral resolution better than 100 nm in some cases [13], its use is limited due to low ion yield. In order to achieve a sensitivity enhancement under Ga^+ bombardment, the measurements were assisted with oxygen flooding ($P= 10^{-6}$ mbar) as described by Frache et al. [14]. A Ga^+ beam focused (25.5 keV) down to 500 nm in diameter with an intensity of 150 pA was scanned across an area of (50×50) μm^2. Elements were analyzed as positive ions. The counting times were 20 s for ^{12}C, ^{24}Mg, ^{28}Si, ^{52}Cr, ^{54}Fe, ^{55}Mn and 40 s for ^{48}Ti, ^{63}Cu, ^{120}Sn and ^{118}Sb. The definition of the images is 256 × 256 pixels. The different images were acquired successively, from the lowest (12 for carbon) to the highest atomic mass (121 for Sb) giving the plane 1 for each element studied. Then new successive series of acquisitions were performed, giving planes 2, 3...8. For elements present as traces (Sb and Sn), the signal obtained for each plane (from 1 to 8 planes) was accumulated in order to increase the statistic of the measurements. For all the other elements present in higher quantities, the signal from only one plane is high enough to be meaningful. It is of note that the SIMS intensity depends on the elements analyzed. As an illustration, from Migeon's data [15], the ionization of Si^+, Cr^+, Cu^+ in steels under Ga^+ bombardment is respectively 80, 2 and 26 times higher than the ionization of Fe. Due to this dependence, it is not possible to compare intensities from one sample to the other without deeper investigations using standard samples to establish a relation between SIMS intensities and concentrations. The detection limit should be about a few tens of ppm for every element, except for carbon which has a lower yield when measured as positive ions.

3. Results

The samples were observed by light microscopy and scanning electron microscopy for studying differences in graphite shape and distribution. Large graphite precipitates were observed attached along the crucible walls, but mainly close to the top surface of the samples. The remaining of the material showed much smaller primary precipitates of graphite and consisted essentially in austenite dendrites and eutectic with undercooled graphite. The large precipitates of graphite may certainly be associated to primary deposition of this phase, suggesting they detached from the crucible walls during the holding at 1180°C and floated due to the density difference between graphite and liquid iron. The remaining of the material shows solidification structures formed after the crucible was drawn out of the furnace. As for the shape and distribution of primary graphite, the largest effects with respect to the reference ferritic alloy were that of Ti which greatly reduced graphite nucleation and growth, and that of Sb which led to rounded agglomerates together with lamellar graphite. This is illustrated in figure 1.

In most cases, the graphite lamellas in the ferritic alloy have smooth edges and a more or less constant thickness that may be indicative of a monotonous growth. Bulk graphite appears smooth as well and no particular feature could be observed at the branching of lamellas. Figure 2 shows an example with SIMS maps of ^{12}C, ^{25}Mg, ^{28}Si, ^{54}Fe and ^{63}Cu for the ferritic alloy. Graphite is observed not to contain any Fe and Cu, but little Si and a very homogeneous distribution of Mg. It is seen that this latter element gives enriched spots containing also Mn, but outside the graphite lamellas. These are certainly oxide particles. Some small Si spots may also be noted at the graphite/matrix interface that may also be oxide particles. It is also observed that the small amount of copper present in this alloy concentrates in the fine eutectic on the upper left of the area that was certainly a last to solidify zone.

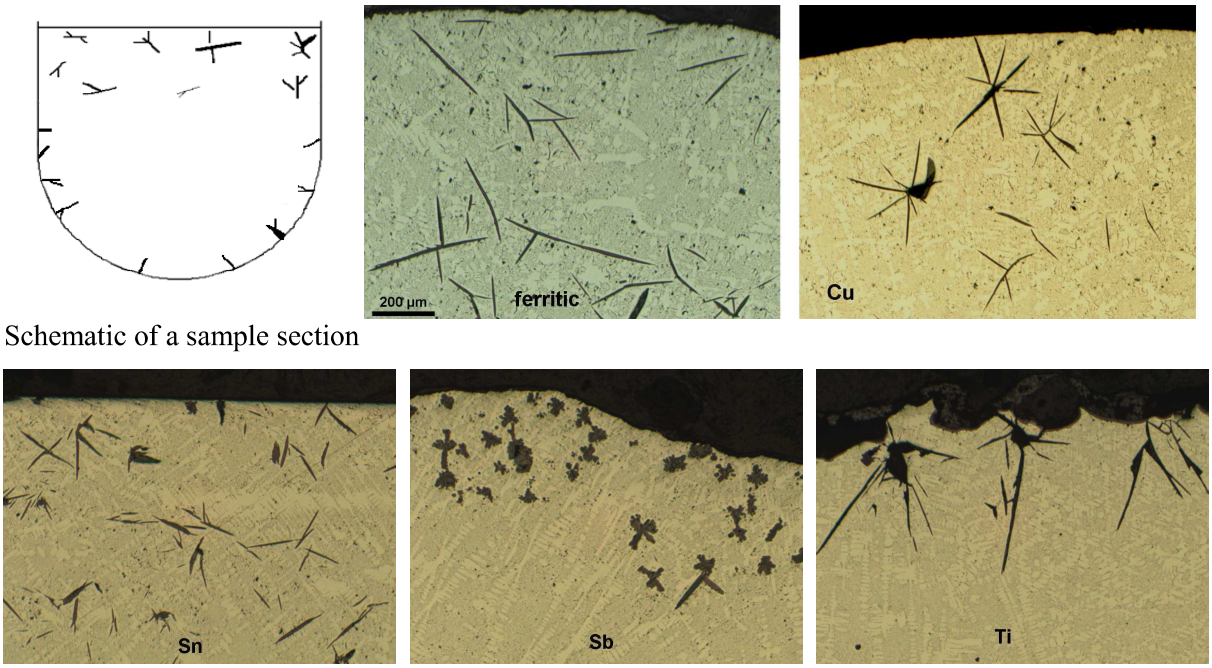

Figure 1. Schematic of a sample section and optical micrographs of the upper sample surface of all five alloys. The scale is the same for all micrographs.

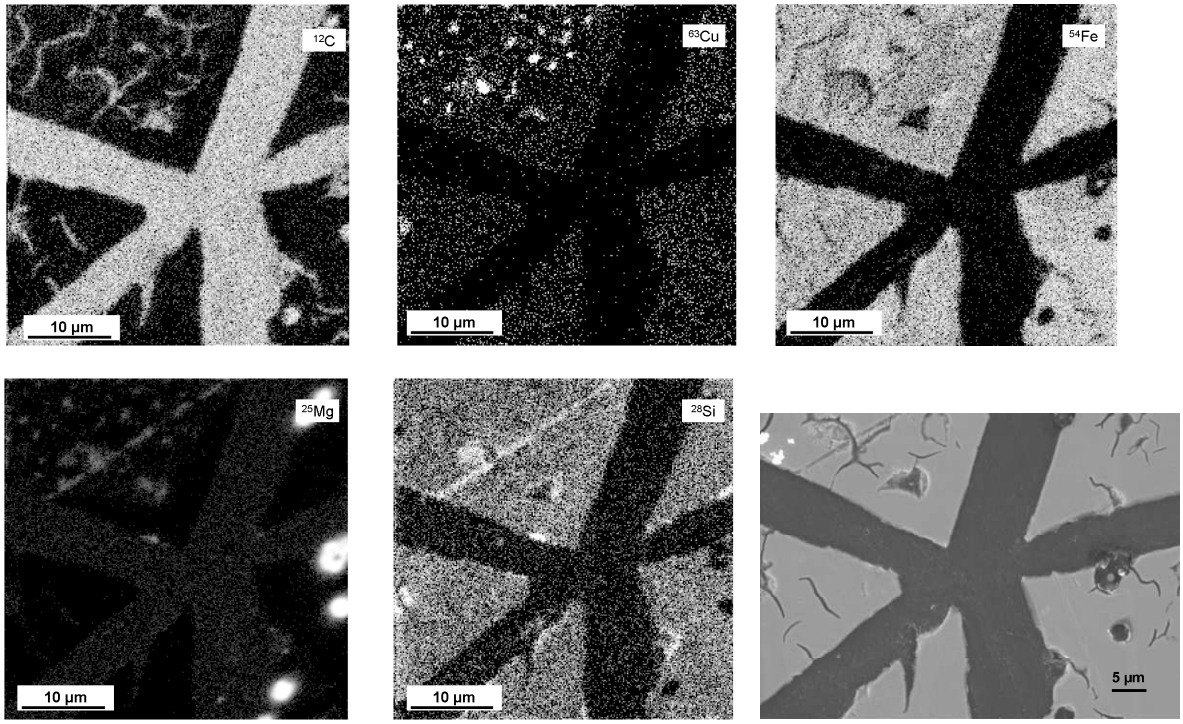

Figure 2. SIMS maps (logarithmic scale) and corresponding SEM micrograph of a graphite precipitate in ferritic alloy 10F2.

In the case of alloy 8P1 that contains Cu and a small amount of Sn, it has been found that the graphite lamellas contain some Fe and Mg generally homogeneously distributed. However, one

complex branching illustrated in figure 3 shows graphite with its surface appearing perturbed on the SEM image and which was found with SIMS to contain lots of metallic elements, mostly as enriched spots. Further, all SIMS analyses performed on this alloy showed Cu and Sn to be essentially evenly distributed in the matrix, i.e. not accumulated at the graphite/matrix interface, apart for some high content spots that may be related to the last to solidify zones as for alloy 10F2 and not to the growth of primary graphite.

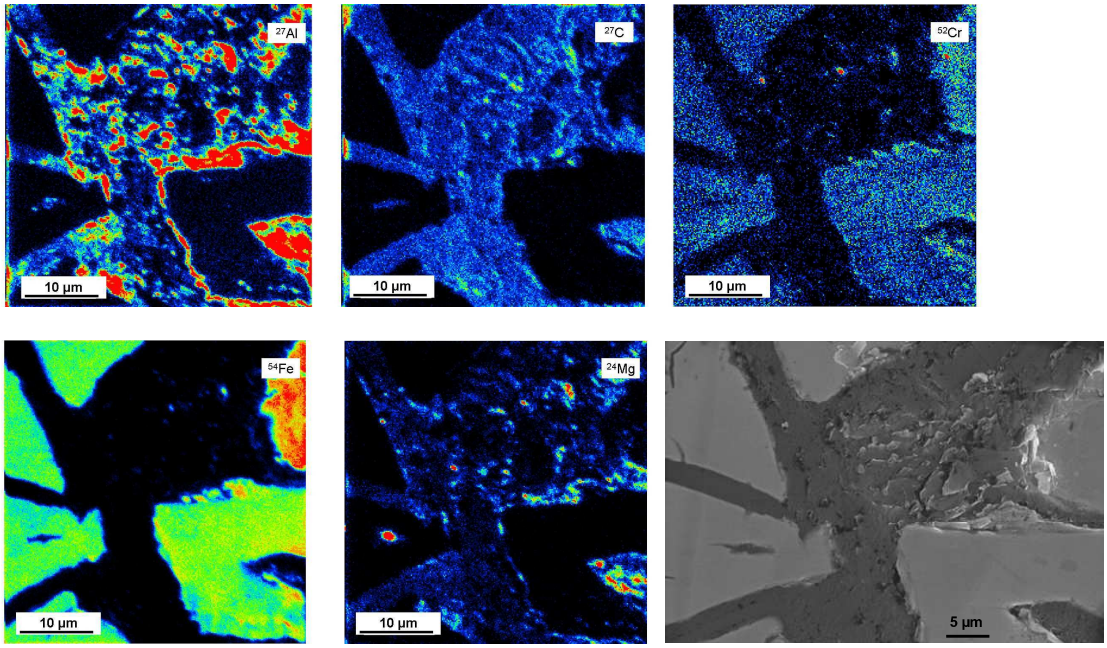

Figure 3. SEM micrograph and SIMS maps (linear scale) of branching lamellas in alloy 8P1.

In alloy 8P3 doped with Sn, it was also noted that many metallic elements (Mg, Cu, Cr, Fe, Si, Al) are present within the graphite, either more or less homogeneously distributed or as spots. It was observed that Sn does not accumulate preferentially in the graphite or at the graphite/matrix interface, whilst some spots were observed that should correspond to oxide particles. Further, it appeared evident that the graphite/matrix interface is much more irregular in this alloy than it is in the two previous ones.

In the case of the Sb-doped alloy, the graphite/matrix interface appears even more perturbed than in alloy 8P3 doped with Sn as illustrated in figure 4. Sb mapping, not shown here, was also performed that showed an even distribution of this element in the matrix and its absence in graphite. In some graphite precipitates, the distribution of metallic elements appeared layered. Moreover, accumulation of Al and Mg was observed at some graphite/matrix interfaces. Finally, it was found that Ti enters within graphite both homogeneously distributed and as spots (certainly oxides) together with most of the other metallic elements (Al, Cr, Cu, Fe, Mg, Mn and Si)

4. Conclusion

As reported, graphite in cast irons contains small but definite amounts of several elements. While their distribution seems homogeneous in general for the ferritic alloy investigated, it was found to be inhomogeneous in the pearlitic grades containing Cu and doped with Sn, Sb and Ti. Further, it was observed that the graphite precipitates in the doped alloys present a disturbed aspect at the junctions between connected lamellas, and a wavy interface with the matrix. These latter observations were mostly marked with addition of Sb, which gives rounded precipitates together with lamellas, and with Sn. It is worth stressing that SIMS mapping did not evidence any build-up of doping elements around graphite precipitates, while some Mg and Al accumulation was sometimes noted. These observations

suggest that additives and trace elements affect graphite growth at an atomic level, e.g. by perturbing its crystalline structure, and do not relate to a morphological instability induced by solute redistribution.

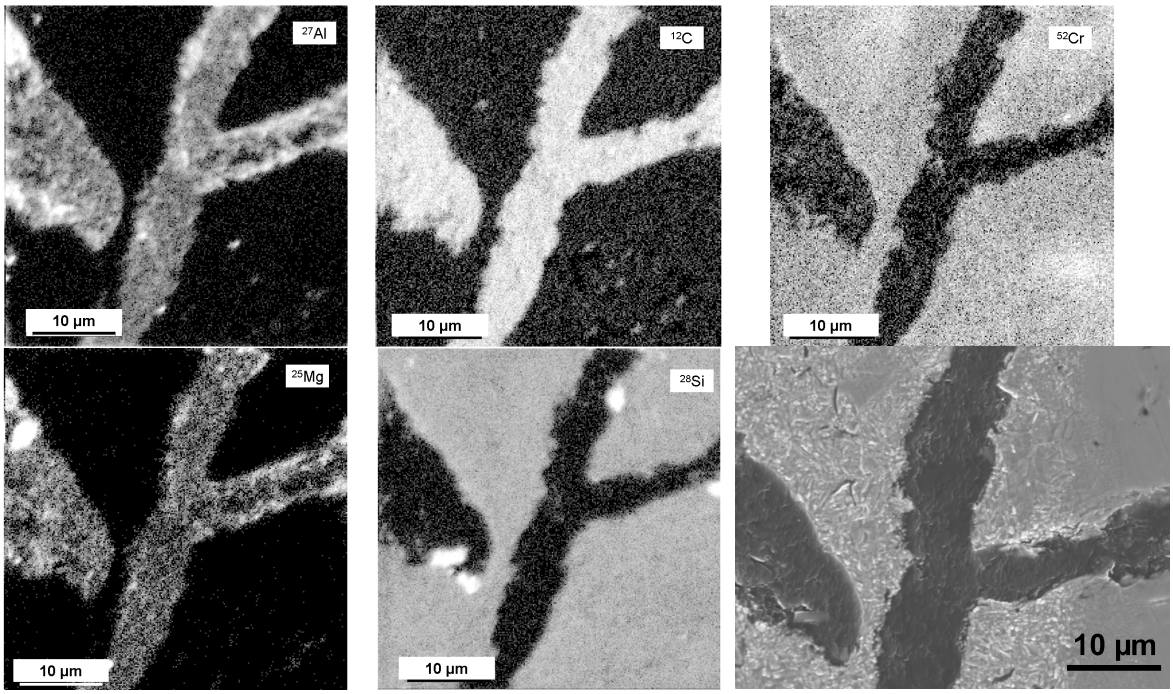

Figure 4. SIMS maps (logarithmic scale) of the Sb-doped alloy and corresponding SEM micrograph.

References

[1] Lux B 1970 *Giessereiforschung in English* **22** 65-81

[2] Merchant H D 1964 *Proc. Recent Research on Cast Iron*, ed H.H. Merchant, ASM (New-York: Gordon and Breach) pp 1-100

[3] Javaid A and Loper C R 1995 *AFS Trans.* **103** 135-50

[4] Karsay S I and Campomanes E 1970 *AFS Trans.* **78** 85-92

[5] Francis B 1979 *Metall. Trans. A* **10A** 21-31

[6] Feng Songlin et al. 1995 *Nuclear instruments and Methods in Physics Research B* **104** 557-60

[7] Feng S L, Ren M Q and Zhong M 1996 *Nuclear instruments and Methods in Physics Research B* **109/110** 584-86

[8] Franklin S E and Stark R A 1984 *Metal Science* **18** 187-200

[9] Franklin S E and Stark R A 1985 *Proc. The Physical Metallurgy of Cast Iron*, ed H. Fradriksson and M. Hillert, Mat. Res. Soc. Symp. Proc. Vol. 34 (New-York: Norh-Holland) pp 25-35

[10] Patterson W, Geilenberg H and Lange B 1974 *Giesserei-Forschung* **26** 121-28

[11] Geilenberg H., Lange B. 1975 *Proc. The Metallurgy of Cast Iron*, ed Lux B., Minkoff I. and Mollard F. (St Saphorin, Switzerland: Georgi Publishing company) pp 529-43

[12] Asenjo I, Lacaze J, Larrañaga P, Méndez S, Sertucha J and Suarez R 2011 *Key Engineering Materials* **457** 52-57

[13] Chabala J M, Levi-Setti R and Wang Y L 1988 *Applied Surface Science* **32** 10-32.

[14] Frache G, El Adib B, Audinot J-N and Migeon H-N 2011 *Surface and interface analysis* **43** 639–642

[15] Migeon H-N, Saldi F, Gao Y and Schuhmacher M 1995 *International Journal of Mass Spectrometry and Ion Processes* **143** issue C 51-63.